

Biliazine: A ring open phthalocyanine analog with a meso hydrogen bond.

Briana R. Schrage,^a Victor N. Nemykin,^b and Christopher J. Ziegler^a

a Department of Chemistry, University of Akron, Akron, Ohio 44312-3601, United States

b Department of Chemistry, University of Manitoba, Winnipeg, Manitoba R3T 2N2, Canada

Supplementary Information

Table of Contents

	Page
General Information	S4-5
Full citation for Gaussian	S6
Syntheses	S7-9
Figure S1: ^1H NMR (500 MHz) of 1 in d6-DMSO.	S10
Figure S2: ^1H NMR (500 MHz) of 5 in d6-DMSO.	S11
Figure S3: $^{13}\text{C}\{^1\text{H}\}$ NMR (125 MHz) of 1 in d6-DMSO.	S12
Figure S4: $^{13}\text{C}\{^1\text{H}\}$ NMR (125 MHz) of 5 in d6-DMSO.	S13
Figure S5: High-resolution ESI mass spectra of 1 .	S14
Figure S6: High-resolution ESI mass spectra of 2 .	S15
Figure S7: High-resolution ESI mass spectra of 3 .	S16
Figure S8: High-resolution ESI mass spectra of 4 .	S17
Figure S9: High-resolution ESI mass spectra of 5 .	S18
Figure S10: Cyclic voltammograms in DMF/0.1 TBAPF ₆ .	S19
Figure S11: B3LYP DFT-predicted frontier orbitals for compounds 2-5 .	S20
Figure S12: Experimental and B3LYP TDDFT-predicted spectra for compounds 2-5 .	S21
Figure S13: B3LYP α -spin relative energies of the frontier orbitals for compounds 2-5 .	S22
Figure S14: B3LYP β -spin relative energies of the frontier orbitals for compounds 2-5 .	S23
Figure S15: UV–Vis and MCD spectra of 5 .	S24
Table S1: X-ray crystal data and structure parameters for compounds 1 and 2 .	S25
Table S2: X-ray crystal data and structure parameters for compounds 3-5 .	S26
Table S3: B3LYP TDDFT-predicted energies and expansion coefficients for compound 2 .	S27
Table S4: B3LYP TDDFT-predicted energies and expansion coefficients for compound 4 .	S28-30
Table S5: B3LYP TDDFT-predicted energies and expansion coefficients for compound 3 .	S31-32

Table S6: B3LYP TDDFT-predicted energies and expansion coefficients for compound 5 .	S33
Table S7: B3LYP DFT optimized geometry of compound 2 .	S34
Table S8: B3LYP DFT optimized geometry of compound 4 .	S35-36
Table S9: B3LYP DFT optimized geometry of compound 3 .	S37
Table S10: B3LYP DFT optimized geometry of compound 5 .	S38-39

General Information

Experimental

All reagents and starting materials were purchased from commercial vendors and used without further purification. DII was synthesized according to previously published procedures.¹ Deuterated solvents were purchased from Cambridge Isotope Laboratories and used as received.

NMR spectra were recorded on 300 MHz and 500 MHz spectrometers and chemical shifts were given in ppm relative to residual solvent resonances (¹H NMR and ¹³C NMR spectra). High-resolution mass spectrometry experiments were performed on a Bruker MicroTOF-III and MicroTOF-qIII instruments. Infrared spectra were collected on Thermo Scientific Nicolet iS5 that was equipped with an iD5 ATR. UV-visible spectra were recorded on a Cary 100 Bio UV-visible spectrometer.

X-ray intensity data were measured on a Bruker CCD-based diffractometer with dual Cu/Mo ImuS microfocus optics (Cu K α radiation, λ = 1.54178 Å, Mo K α radiation, λ = 0.71073 Å). Crystals were mounted on a cryoloop using Paratone oil and placed under a stream of nitrogen at 100 K (Oxford Cryosystems). The detector was placed at a distance of 5.00 cm from the crystal. The data were corrected for absorption with the SADABS program. The structures were refined using the Bruker SHELXTL Software Package (Version 6.1),² and were solved using direct methods until the final anisotropic full-matrix, least squares refinement of F² converged.

Electrochemistry measurements were conducted using a CHI 820D potentiostat in a standard three-electrode configuration. Platinum wire was used as the counter electrode. The working electrode used was a 2 mm diameter platinum disk. A nonaqueous Ag/Ag⁺ reference electrode was used by immersing silver wire in a degassed DMF solution of 0.01 M AgNO₃ / 0.1 M tetrabutylammonium hexafluorophosphate (TBAPF₆). All potentials were referenced to the

ferrocene/ferrocenium couple. The concentration of analyte was 1.0 mM, and the supporting electrolyte was 0.1 M TBAPF₆ dissolved in DMF.

Computational Details

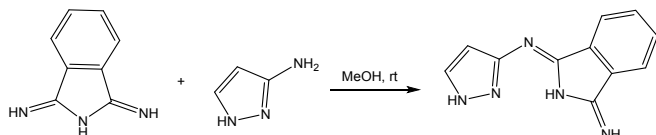
The starting geometries of compounds **1** and **3** were optimized using a B3LYP exchange–correlation functional.³ Energy minima in optimized geometry were confirmed by the frequency calculations (absence of the imaginary frequencies). The solvent effect was modeled using the polarized continuum model (PCM).⁴ In all calculations, CHCl₃ was used as the solvent. In PCM-TDDFT calculation, the first 50 states were calculated. All atoms were modeled using the 6-311G(d)⁵ basis set. Gaussian 09 software was used in all calculations.⁶ The QMForge program was used for molecular orbital analysis in all cases.⁷

Full citation for Gaussian

Gaussian 09, Revision D.01, Frisch, M. J.; Trucks, G. W.; Schlegel, H. B.; Scuseria, G. E.; Robb, M. A.; Cheeseman, J. R.; Montgomery, Jr., J. A.; Vreven, T.; Kudin, K. N.; Burant, J. C.; Millam, J. M.; Iyengar, S. S.; Tomasi, J.; Barone, V.; Mennucci, B.; Cossi, M.; Scalmani, G.; Rega, N.; Petersson, G. A.; Nakatsuji, H.; Hada, M.; Ehara, M.; Toyota, K.; Fukuda, R.; Hasegawa, J.; Ishida, M.; Nakajima, T.; Honda, Y.; Kitao, O.; Nakai, H.; Klene, M.; Li, X.; Knox, J. E.; Hratchian, H. P.; Cross, J. B.; Adamo, C.; Jaramillo, J.; Gomperts, R.; Stratmann, R. E.; Yazyev, O.; Austin, A. J.; Cammi, R.; Pomelli, C.; Ochterski, J. W.; Ayala, P. Y.; Morokuma, K.; Voth, G. A.; Salvador, P.; Dannenberg, J. J.; Zakrzewski, V. G.; Dapprich, S.; Daniels, A. D.; Strain, M. C.; Farkas, O.; Malick, D. K.; Rabuck, A. D.; Raghavachari, K.; Foresman, J. B.; Ortiz, J. V.; Cui, Q.; Baboul, A. G.; Clifford, S.; Cioslowski, J.; Stefanov, B. B.; Liu, G.; Liashenko, A.; Piskorz, P.; Komaromi, I.; Martin, R. L.; Fox, D. J.; Keith, T.; Al-Laham, M. A.; Peng, C. Y.; Nanayakkara, A.; Challacombe, M.; Gill, P. M. W.; Johnson, B.; Chen, W.; Wong, M. W.; Gonzalez, C.; Pople, J. A. Gaussian, Inc., Wallingford CT, 2009.

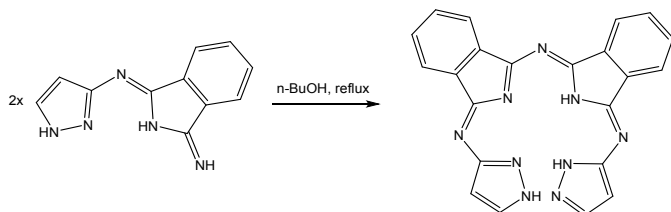
Syntheses.

Synthesis of 1. 1,3-Diiminoisoindoline (1.00 g, 6.89 mmol) and 3-amino pyrazole (0.57 g, 6.89 mmol) were dissolved in methanol (20 mL) and stirred at room temperature for 1 hour. The resultant solid was filtered, washed with cold methanol, and air dried to give a yellow solid. Crystals suitable for X-ray diffraction were grown by slow evaporation from DMF.



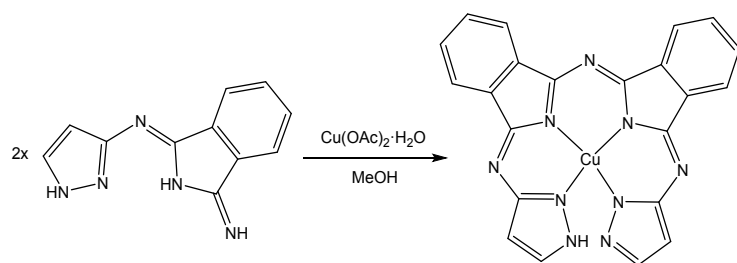
1: Yield: 1.16 g (79.6%). ^1H NMR (300 MHz, d_6 - DMSO): δ = 12.66 (s, 1H), 8.70 (s, 2H), 7.90 (d, J = 7.0 Hz, 1H), 7.76 (d, J = 6.7 Hz, 1H), 7.57 (m, 2H), 7.47 (s, 1H), 6.64 (s, 1H). $^{13}\text{C}\{^1\text{H}\}$ NMR (125 MHz, d_6 - DMSO): δ = 170.2, 163.8, 140.7, 134.4, 131.1, 129.9, 121.2, 100.5. HRMS (ESI-TOF, positive mode) m/z : calcd for $\text{C}_{11}\text{H}_{10}\text{N}_5$ 212.0931, found 212.0935 $[\text{M}+\text{H}]^+$.

Synthesis of H_2BlzH (2). Compound **1** (0.10 g, 2.37 mmol) was dissolved in *n*-butanol (7 mL) and heated to a reflux for 1 hour. The resultant solid was filtered, washed with cold *n*-butanol, and air dried to give a red solid. Crystals suitable for X-ray diffraction were grown by slow evaporation from DMF.

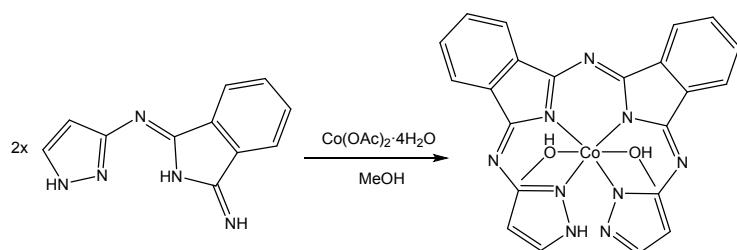


H_2BlzH (2): Yield: 0.088 g (91.5%). HRMS (ESI-TOF, positive mode) m/z : calcd for $\text{C}_{22}\text{H}_{15}\text{N}_9\text{Na}$ 428.1343, found 428.1346 $[\text{M}+\text{Na}]^+$.

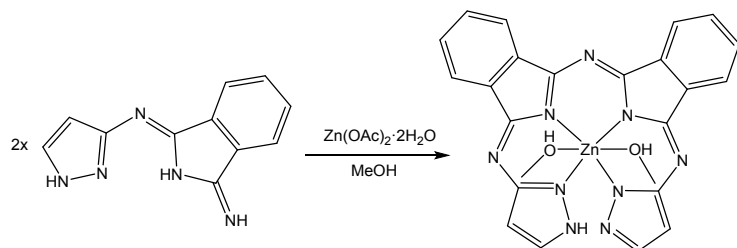
Synthesis of MBlzH complexes. A solution of $M(\text{OAc})_2$ hydrate ($M = \text{Co}, \text{Cu}, \text{Zn}$) (0.12 mmol), and two equivalents of **1** (0.05 g, 0.24 mmol) in MeOH (4.00 mL) were heated until all of the solids dissolved. The mixture was then stirred at room temperature for 1 hour. The resultant precipitate was filtered and washed with cold MeOH. The compounds were isolated as brown $(\text{Co}(\text{BlzH})(\text{MeOH})_2)$ (**4**), and red $(\text{Cu}(\text{BlzH}))$ (**3**) and $\text{Zn}(\text{BlzH})(\text{MeOH})_2$ (**5**) solids. Crystals suitable for X-ray diffraction were grown by slow evaporation of MeOH $(\text{Co}(\text{BlzH})(\text{MeOH})_2)$, and $\text{Zn}(\text{BlzH})(\text{MeOH})_2$, and slow evaporation of THF $(\text{Cu}(\text{BlzH}))$.



Cu(BlzH) (3): Yield: 0.050 g (91.0%). HRMS (ESI-TOF, positive mode) m/z : calcd for $C_{22}H_{14}CuN_9$ 467.0663, found 467.0646 $[M+H]^+$.



Co(BlzH)(MeOH)₂ (4): Yield: 0.049 g (78.3%). HRMS (ESI-TOF, positive mode) m/z : calcd for $C_{22}H_{14}CoN_9$ 463.0699, found 463.0681 $[M+H]^+$.



Zn(BlzH)(MeOH)₂ (5): Yield: 0.052 g (82.2%). 1H NMR (500 MHz, d_6 -DMSO): δ = 16.73 (s, NH), 8.17 (m, 2H), 7.99 (m, 1H), 7.77 (m, 2H), 7.72 (m, 4H), 7.53 (d, J = 1.3 Hz, 2H), 6.63 (d, J = 1.3 Hz, 2H), 4.06 (q, J = 5.3 Hz, CH_3OH), 3.17 (d, J = 5.0 Hz, CH_3OH). $^{13}C\{^1H\}$ NMR (125 MHz, d_6 -DMSO): δ = 172.8, 157.8, 156.0, 140.4, 138.7, 131.7, 130.6, 122.4, 121.6, 107.1. HRMS (ESI-TOF, positive mode) m/z : calcd for $C_{22}H_{14}N_9Zn$ 468.0658, found 468.0665 $[M+H]^+$.

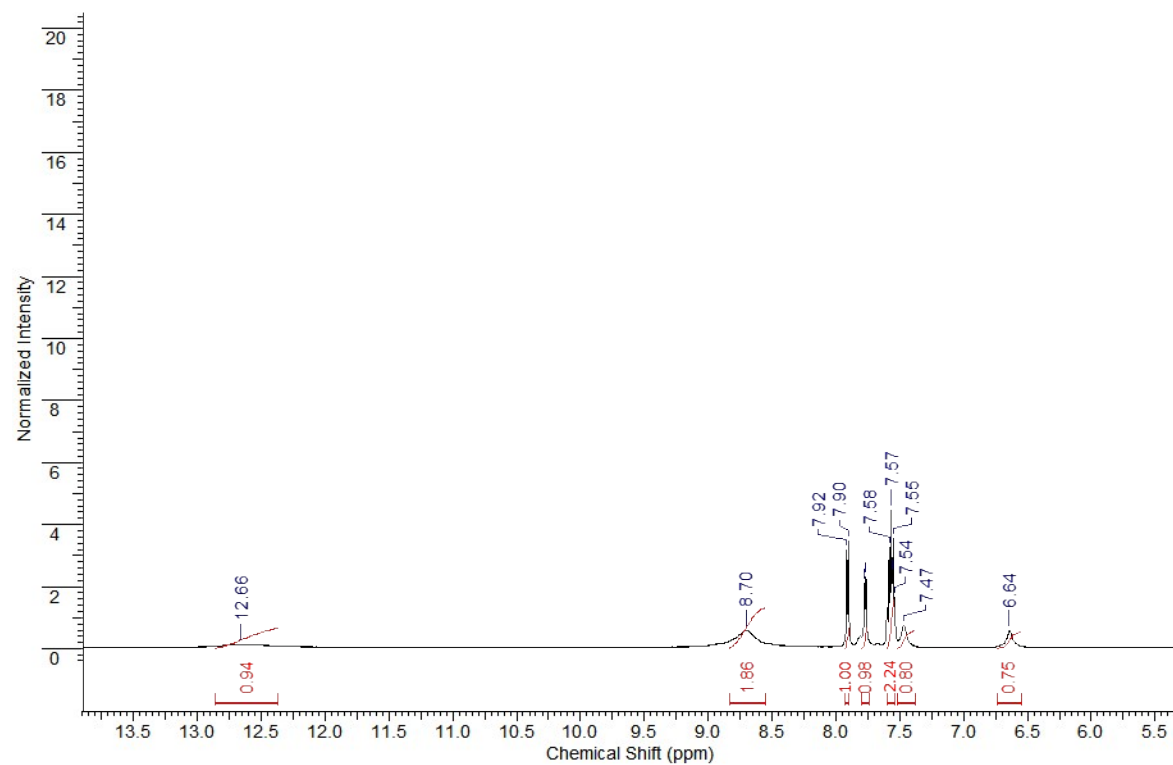
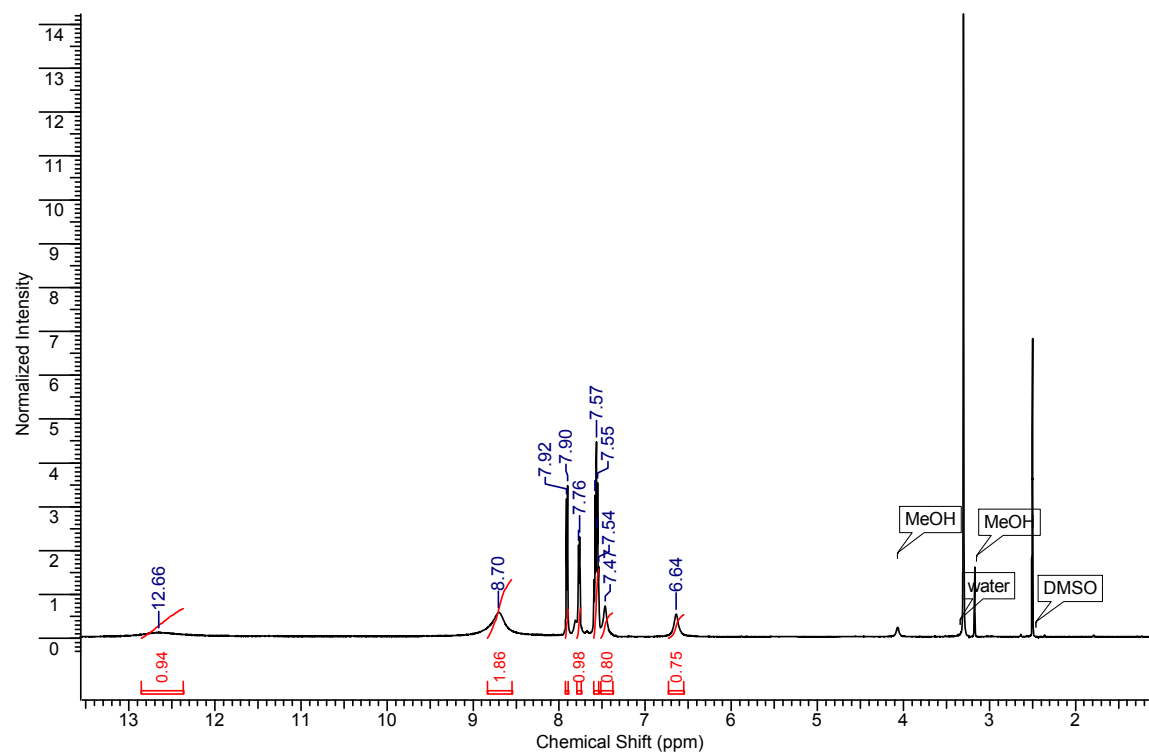


Figure S1: ¹H NMR (500 MHz) of **1** in d₆-DMSO.

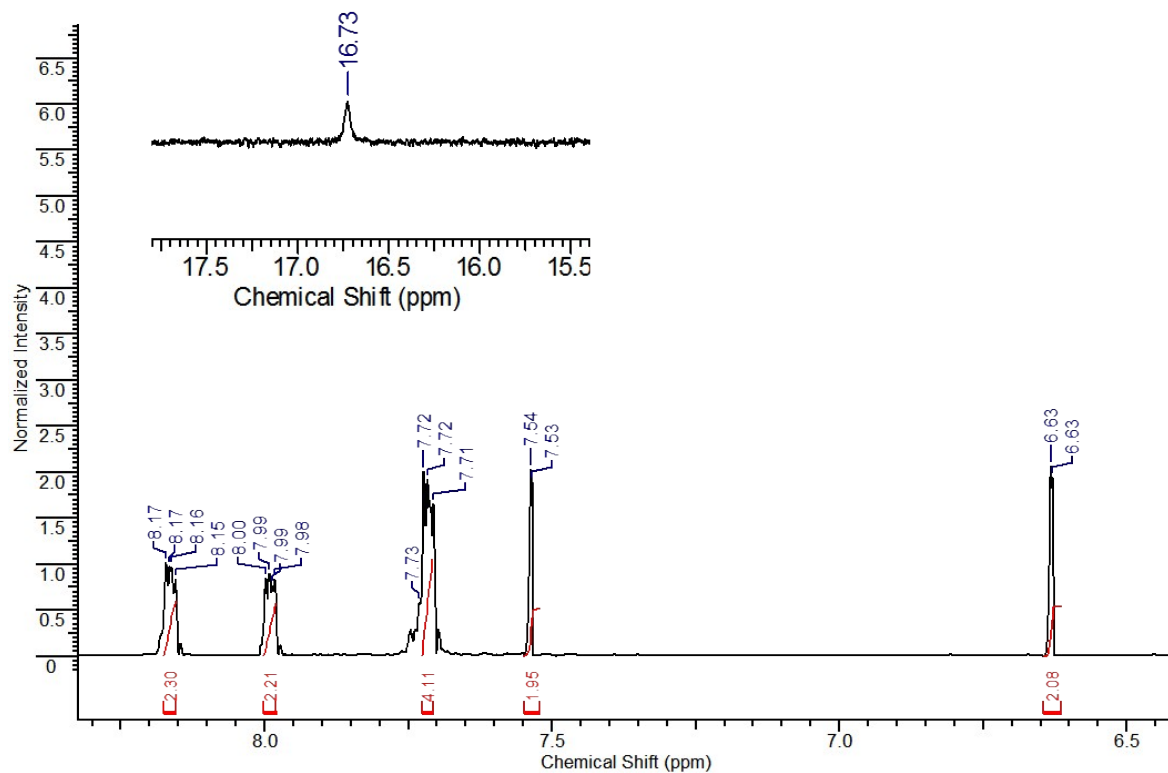
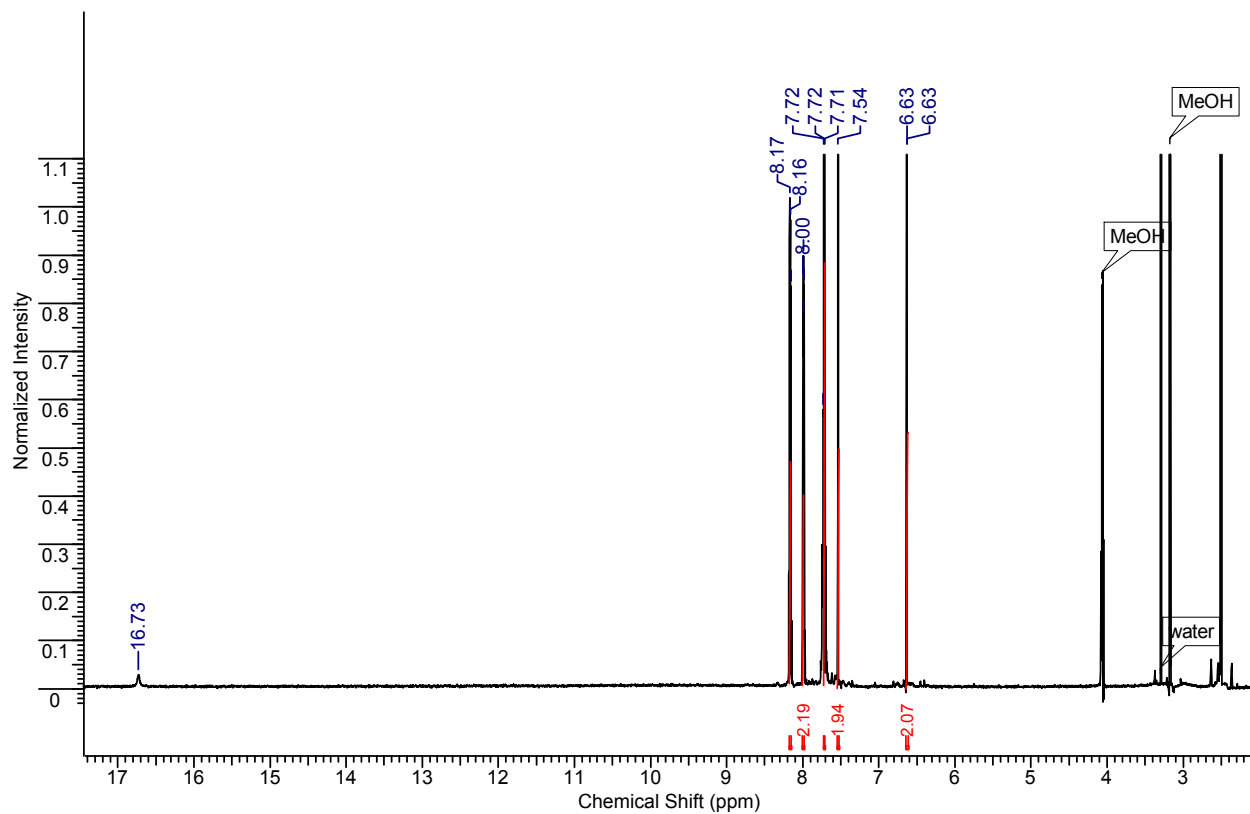


Figure S2: ^1H NMR (500 MHz) of **5** in $\text{d}_6\text{-DMSO}$.

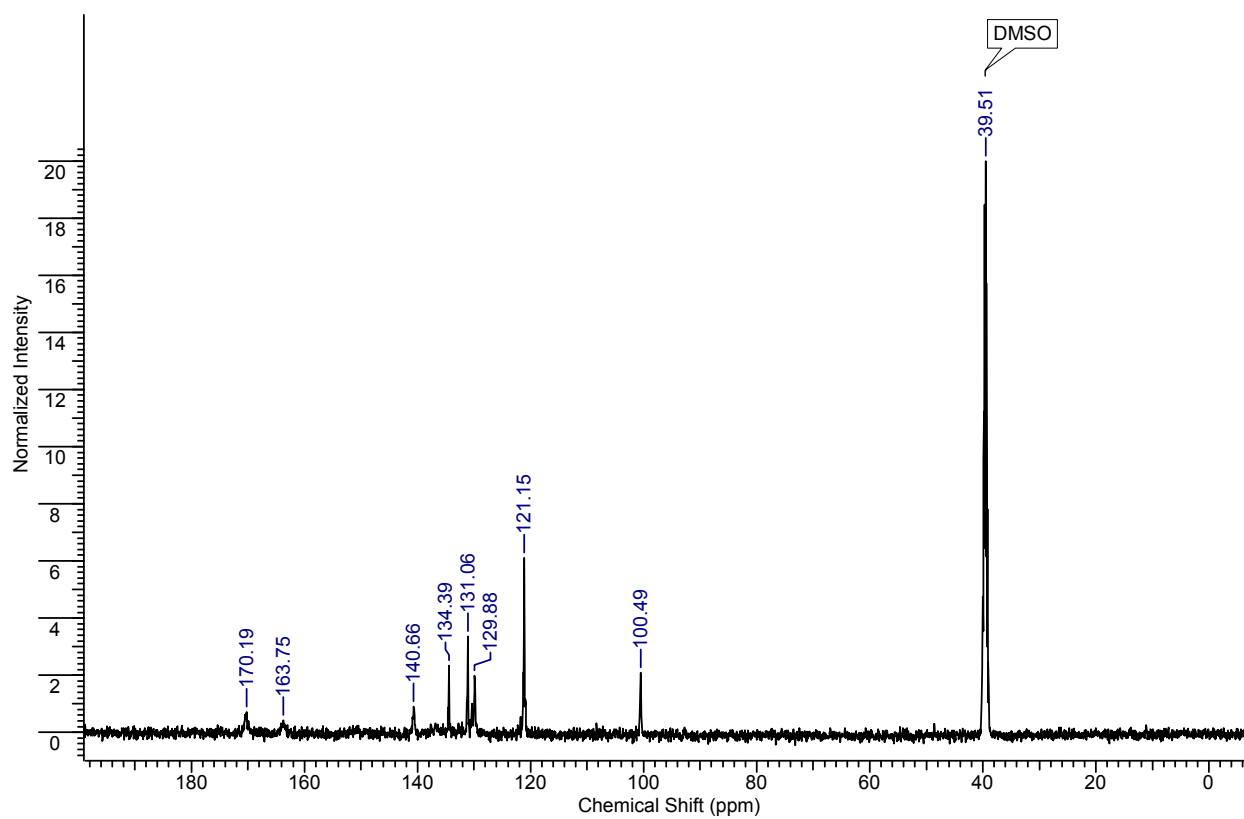


Figure S3: $^{13}\text{C}\{^1\text{H}\}$ NMR (125 MHz) of **1** in $\text{d}_6\text{-DMSO}$.

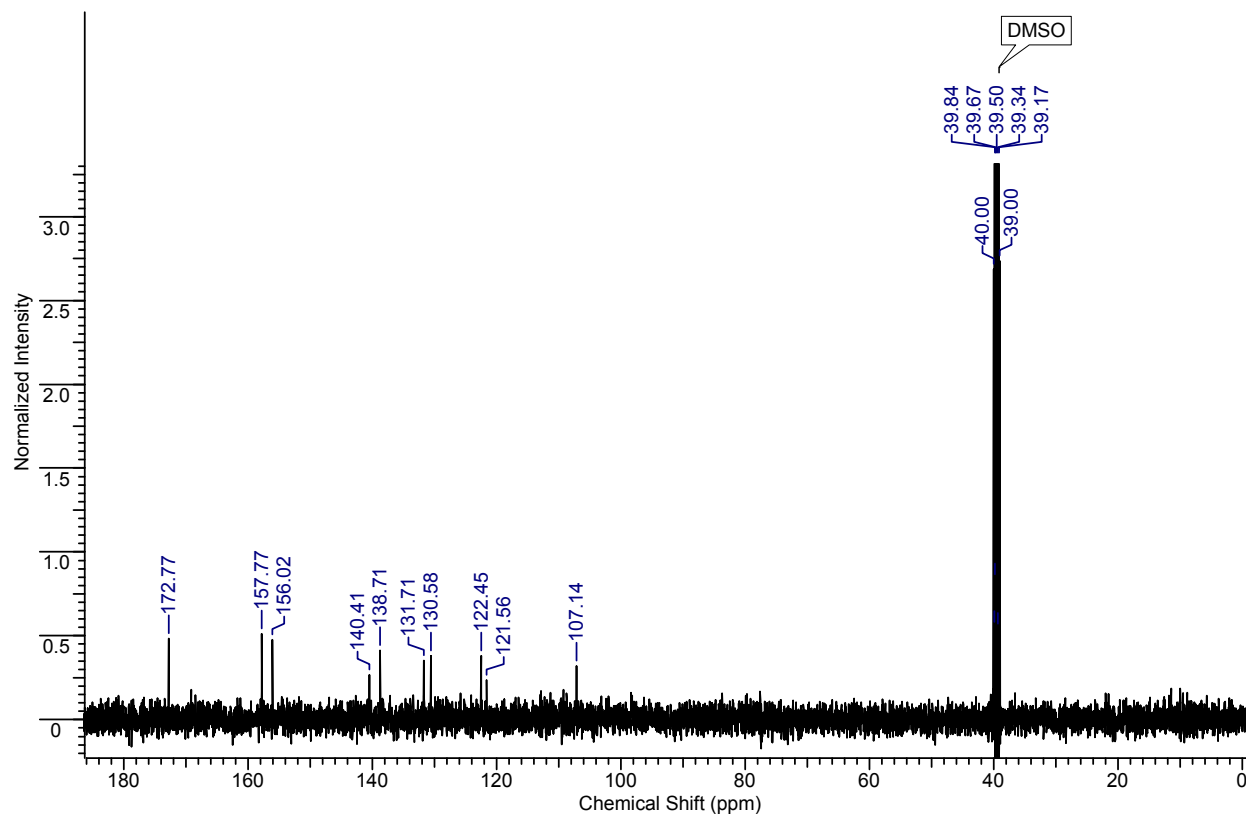


Figure S4: $^{13}\text{C}\{^1\text{H}\}$ NMR (125 MHz) of **5** in $\text{d}_6\text{-DMSO}$.

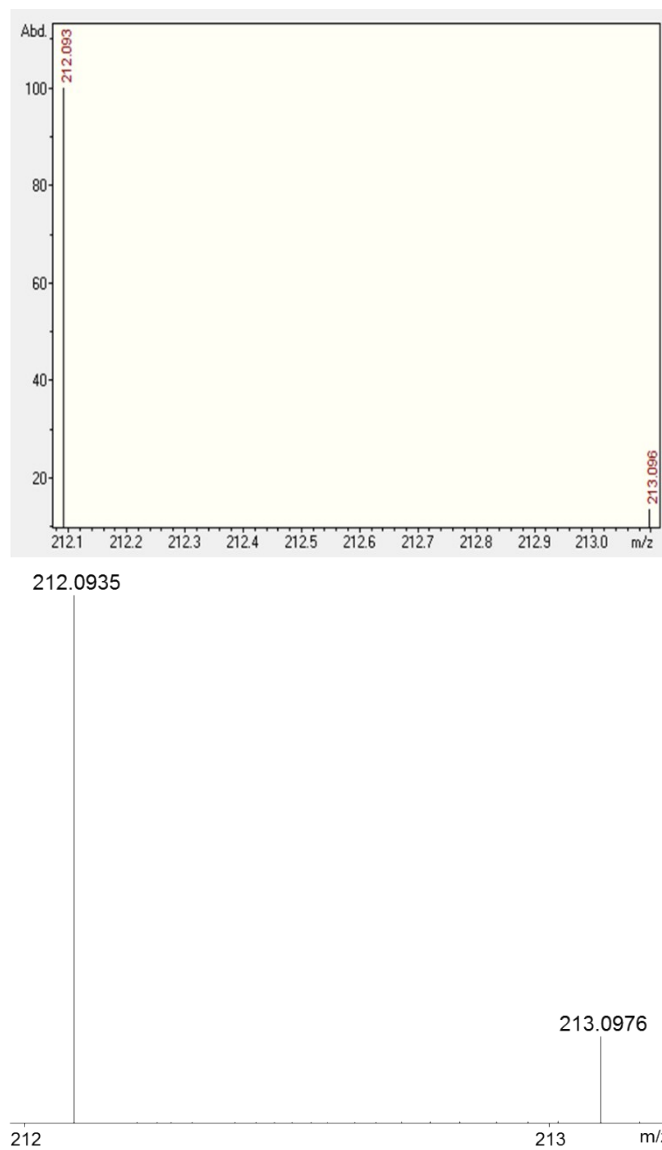


Figure S5: High-resolution ESI mass spectra of **1**. Top: calculated spectrum. Bottom: experimental spectrum.

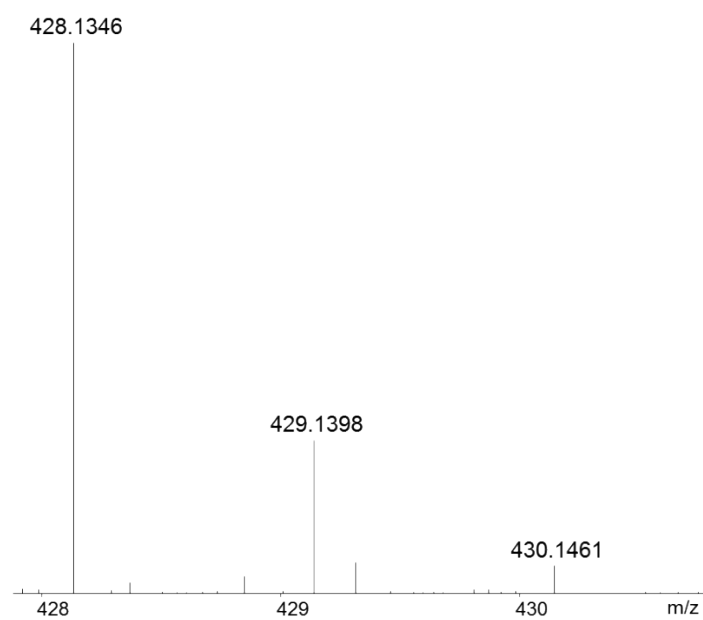
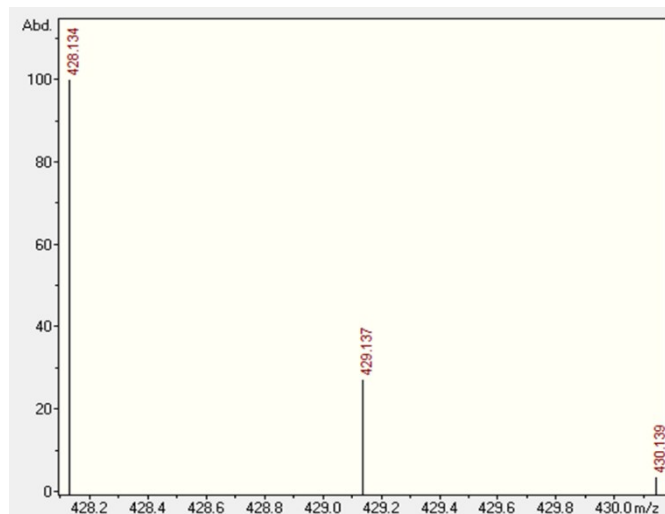


Figure S6: High-resolution ESI mass spectra of **2**. Top: calculated spectrum. Bottom: experimental spectrum.

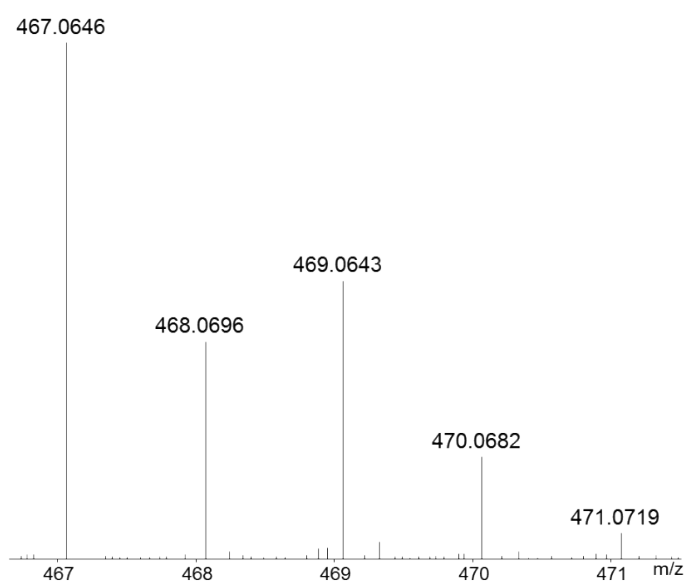
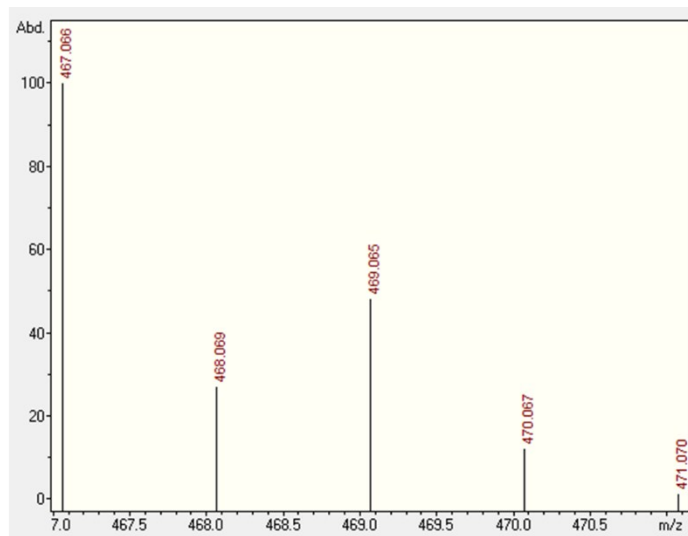


Figure S8: High-resolution ESI mass spectra of **3**. Top: calculated spectrum. Bottom: experimental spectrum.

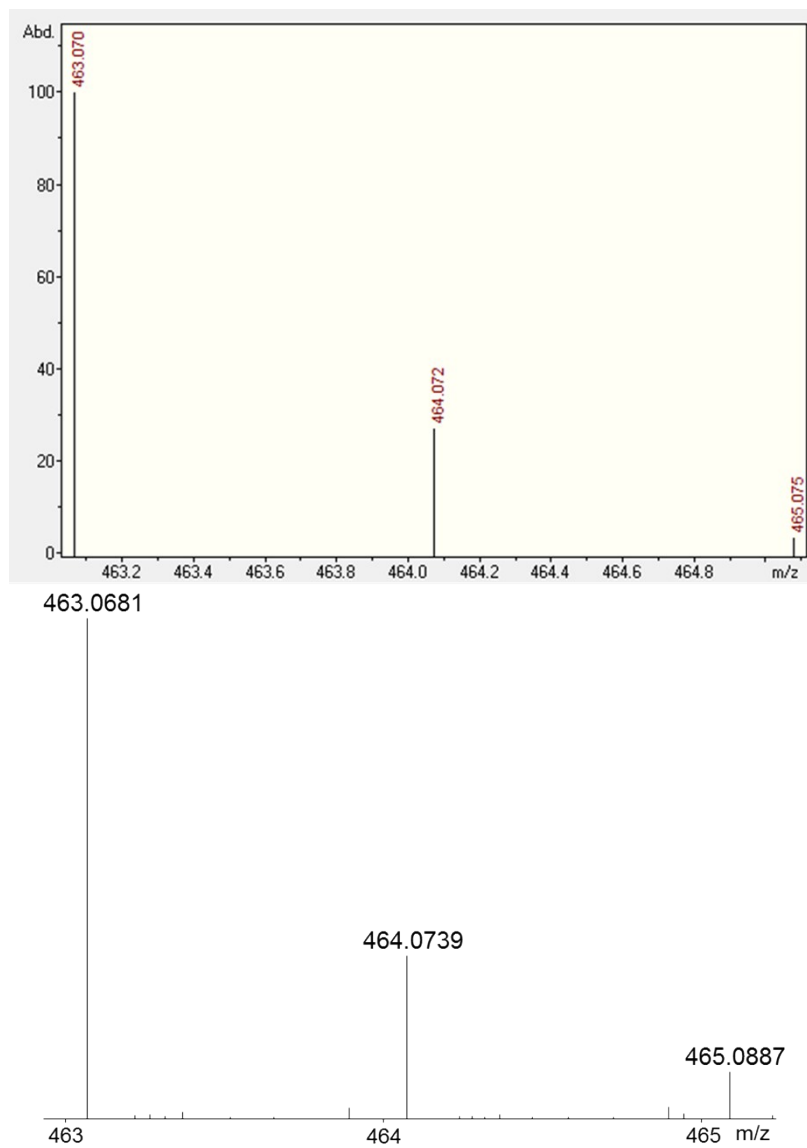


Figure S7: High-resolution ESI mass spectra of **4**. Top: calculated spectrum. Bottom: experimental spectrum.

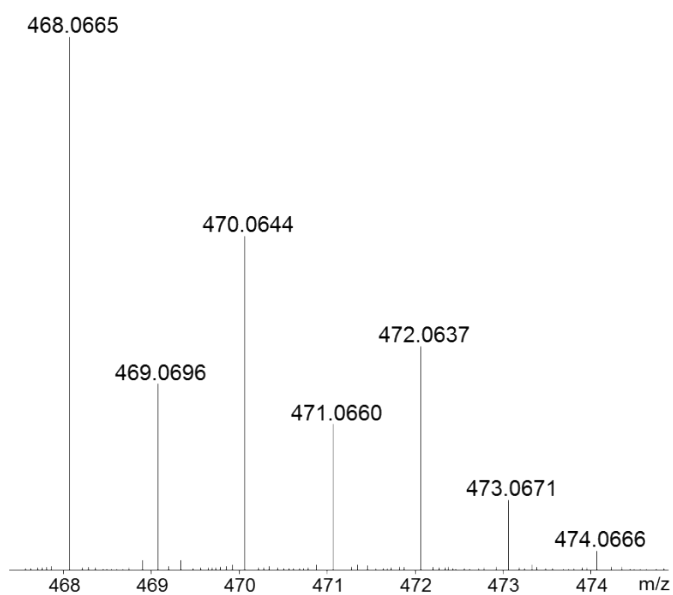
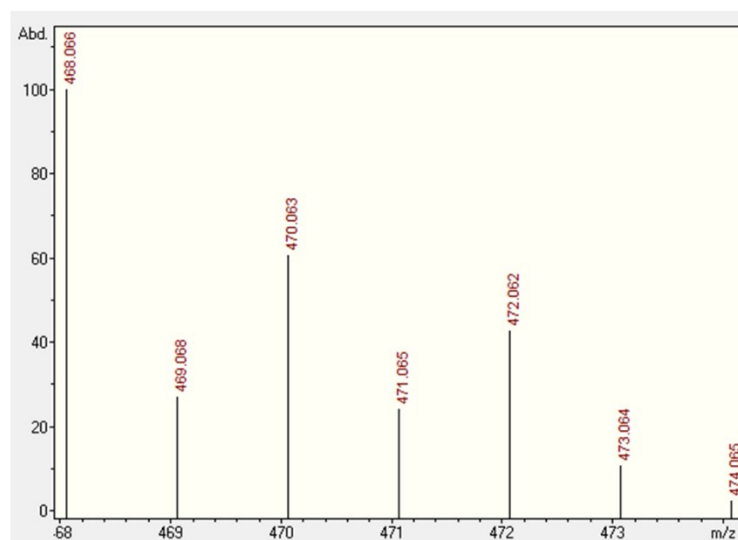


Figure S9: High-resolution ESI mass spectra of **5**. Top: calculated spectrum. Bottom: experimental spectrum.

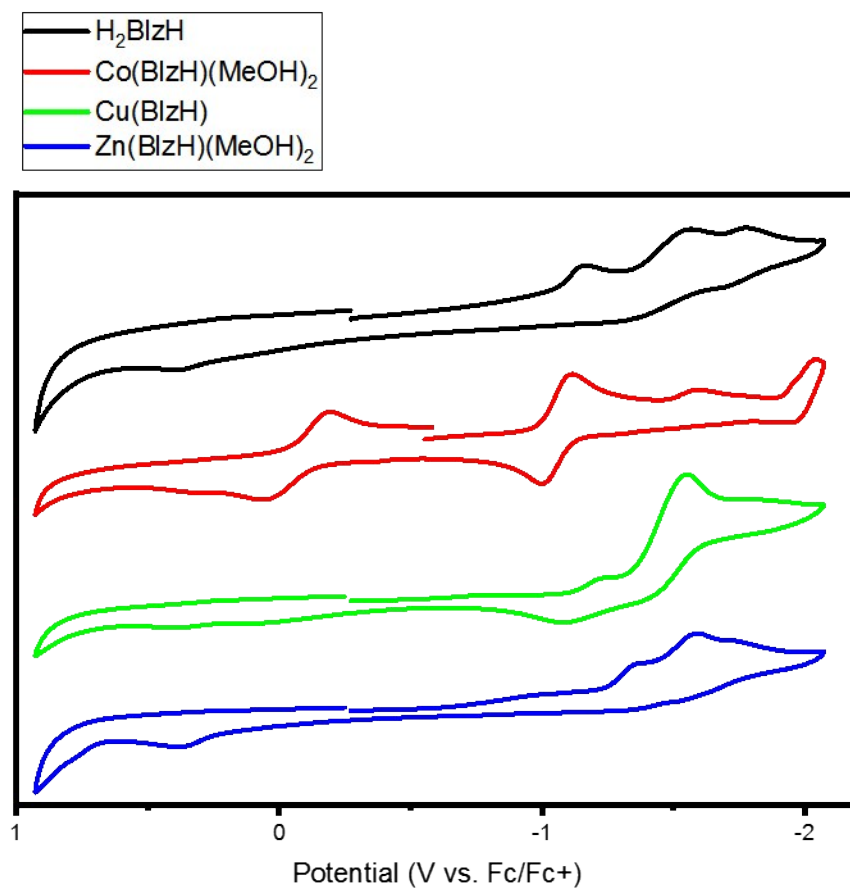


Figure S10: Cyclic voltammograms in DMF/0.1 TBAPF₆.

Compound

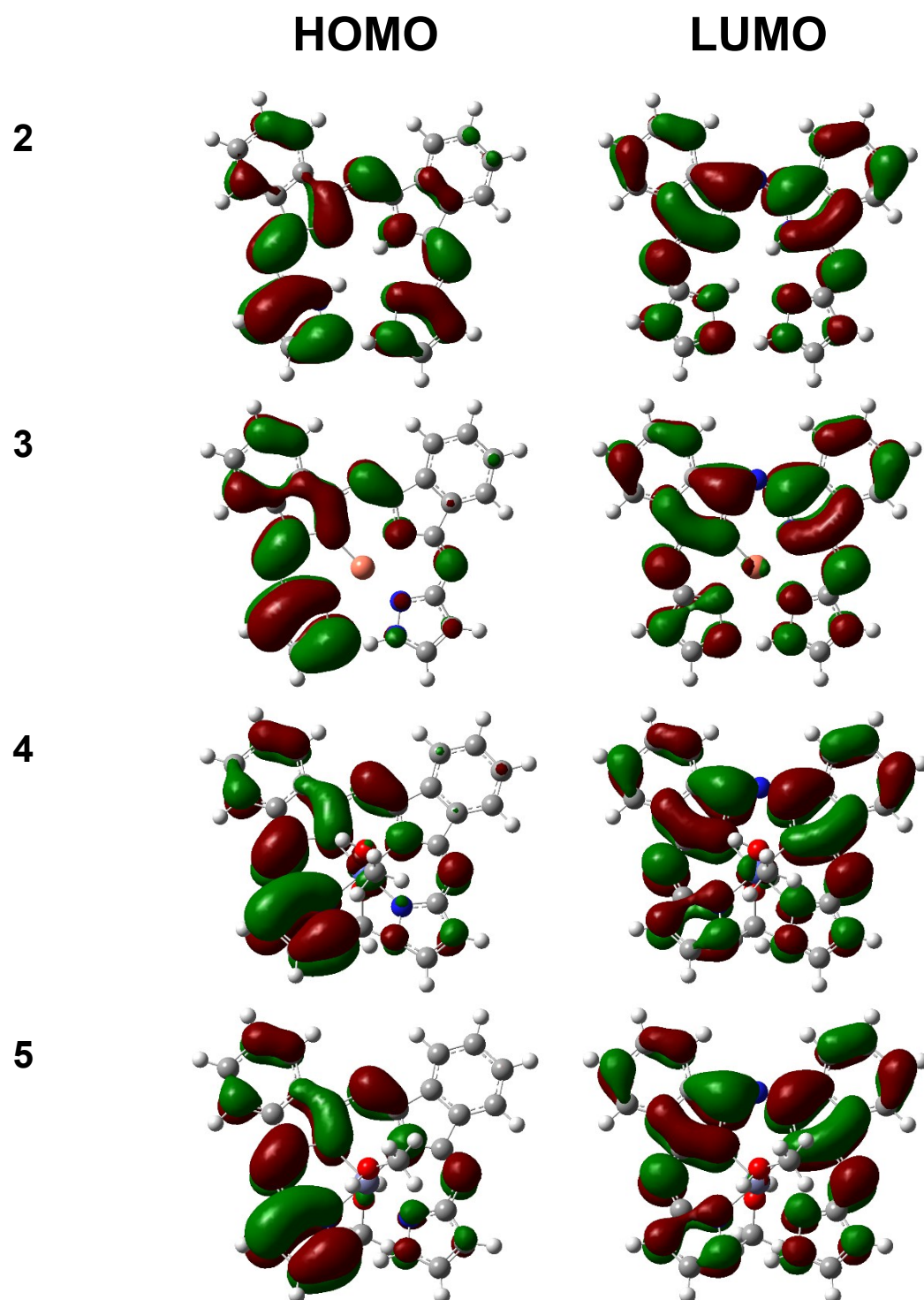


Figure S11. B3LYP DFT-predicted frontier orbitals for compounds 2-5.

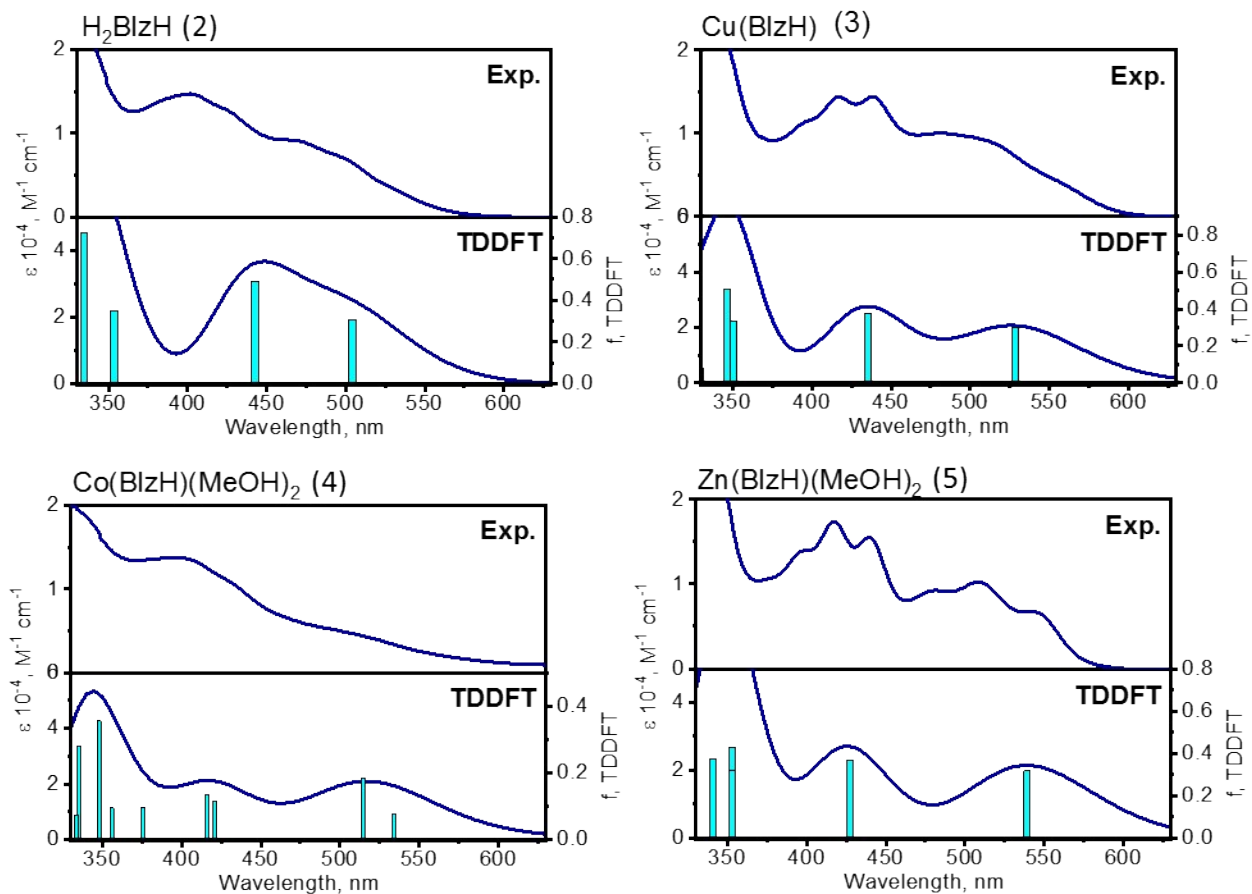


Figure S12: Experimental and B3LYP TDDFT-predicted spectra for compounds 2-5.

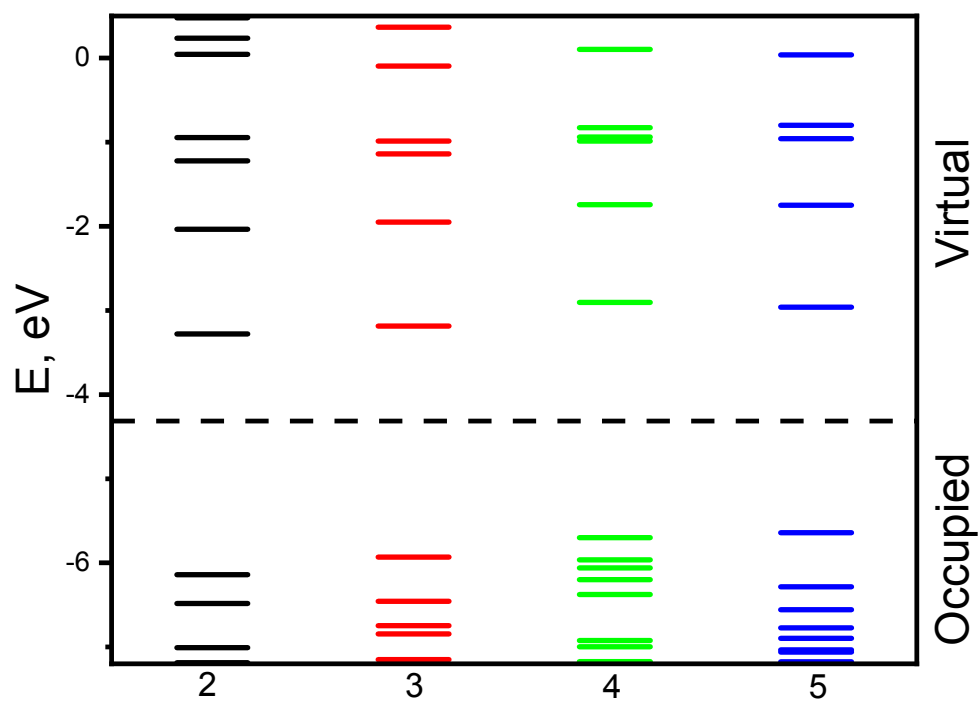


Figure S13: B3LYP α -spin relative energies of the frontier orbitals for compounds 2-5.

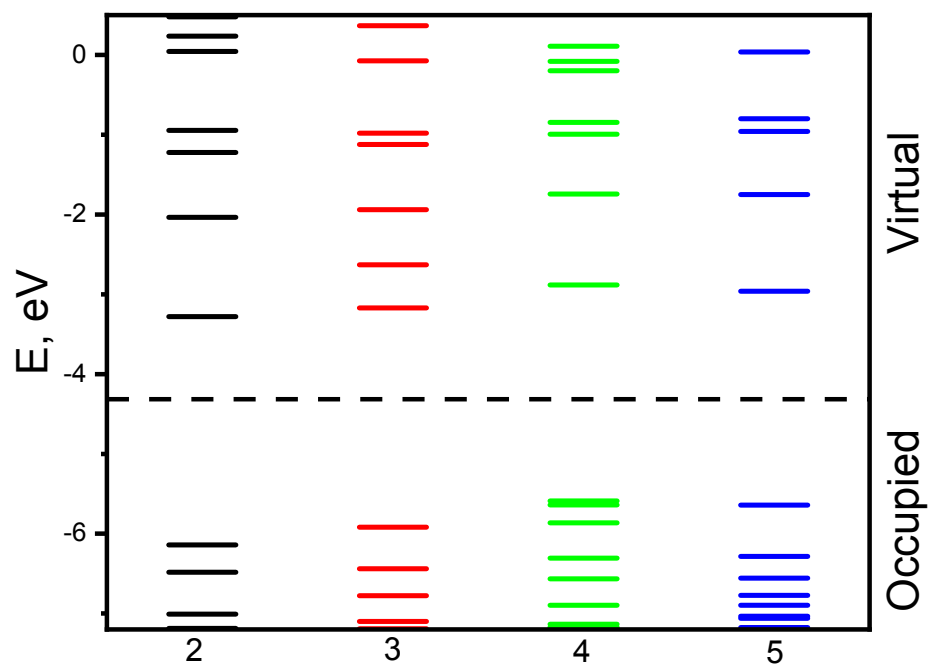


Figure S14: B3LYP β -spin relative energies of the frontier orbitals for compounds 2-5.

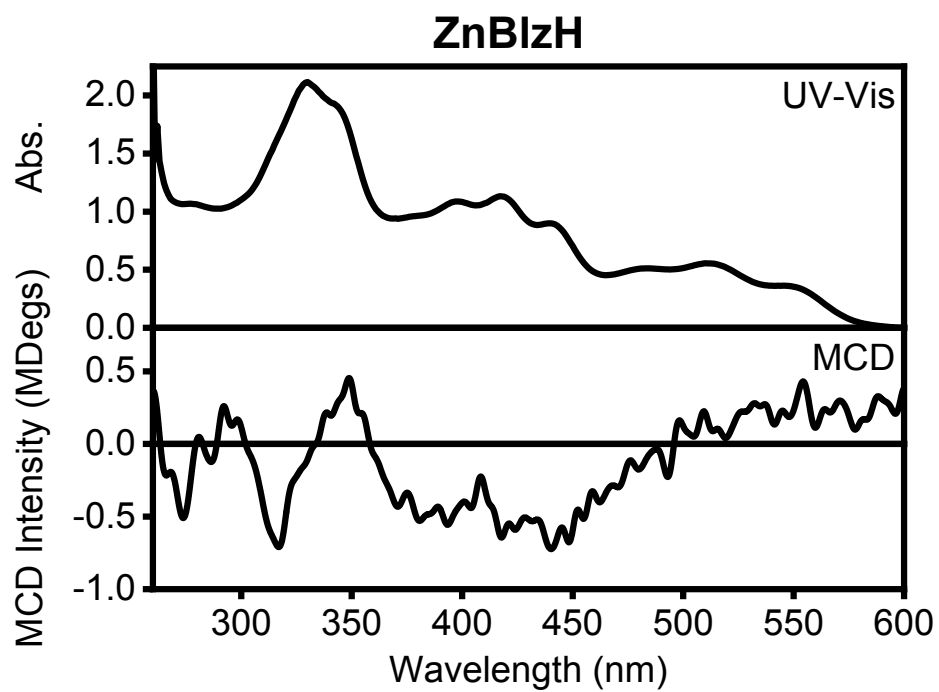


Figure S15: UV-Vis and MCD spectra of **5**.

Table S1: X-ray crystal data and structure parameters for compounds **1** and **2**.

Compound	1	2
Empirical formula	C ₁₁ H ₉ N ₅	C ₂₂ H ₁₅ N ₉
Formula weight	211.23	405.43
Crystal system	Monoclinic	Monoclinic
Space group	C2/c	P2 ₁ /n
a/ Å	11.6141(5)	4.579(6)
b/ Å	12.7038(5)	17.112(13)
c/ Å	13.4922(6)	23.460(16)
α(°)	90	92
β(°)	99.080(3)	93.02(8)
γ(°)	90	90
Volume (Å³)	1965.74(15)	1836(3)
Z	8	4
D_c (Mg/m³)	1.427	1.467
μ (mm⁻¹)	0.757	0.772
F(000)	880	840
reflns collected	6403	11216
indep. reflns	1687	3125
GOF on F²	1.046	1.015
R1 (on F_o², I > 2σ(I))	0.0461	0.0674
wR2 (on F_o², I > 2σ(I))	0.1266	0.1725
R1 (all data)	0.0530	0.1127
wR2 (all data)	0.1336	0.1976

Table S2: X-ray crystal data and structure parameters for compounds **3-5**.

Compound	3	4	5
Empirical formula	C ₂₂ H ₁₃ CuN ₉	C ₂₄ H ₂₁ CoN ₉ O ₂	C ₂₄ H ₂₁ N ₉ O ₂ Zn
Formula weight	466.95	526.43	532.87
Crystal system	Monoclinic	Monoclinic	Monoclinic
Space group	P2 ₁ /n	P2 ₁ /c	P2 ₁ /c
a/ Å	4.6467(4)	6.8635(3)	6.8862(4)
b/ Å	16.7271(17)	23.0498(13)	23.1744(14)
c/ Å	23.289(2)	14.1576(8)	14.2313(8)
α(°)	90	90	90
β(°)	92.885(7)	102.251(3)	102.434(4)
γ(°)	90	90	90
Volume (Å³)	1807.9(3)	2188.8(2)	2217.8(2)
Z	4	4	4
Dc (Mg/m³)	1.716	1.598	1.596
μ (mm⁻¹)	1.994	6.531	1.153
F(000)	948	1084	1096
reflns collected	8721	11209	21335
indep. reflns	2876	3325	5523
GOF on F²	1.008	1.050	1.048
R1 (on F_o², I > 2σ(I))	0.0490	0.0468	0.0511
wR2 (on F_o², I > 2σ(I))	0.1239	0.1159	0.1083
R1 (all data)	0.0851	0.0590	0.0910
wR2 (all data)	0.1454	0.1228	0.1229

Table S3: B3LYP TDDFT-predicted energies and expansion coefficients for compound **2** (only excited states with $f > 0.05$ and $\lambda > 270$ nm are listed).

Excited State 1:	Singlet-A	2.4592 eV	504.17 nm	$f=0.3090$	$\langle S^{*2} \rangle=0.000$
105 ->106	0.70100				
Excited State 2:	Singlet-A	2.8023 eV	442.43 nm	$f=0.4910$	$\langle S^{*2} \rangle=0.000$
104 ->106	0.69021				
105 ->107	0.10982				
Excited State 6:	Singlet-A	3.5049 eV	353.75 nm	$f=0.3514$	$\langle S^{*2} \rangle=0.000$
101 ->106	0.69603				
Excited State 10:	Singlet-A	3.7046 eV	334.67 nm	$f=0.7245$	$\langle S^{*2} \rangle=0.000$
96 ->106	-0.22629				
105 ->107	0.65249				
Excited State 11:	Singlet-A	3.9610 eV	313.01 nm	$f=0.1170$	$\langle S^{*2} \rangle=0.000$
96 ->106	-0.47194				
104 ->107	0.48817				
105 ->107	-0.10861				
Excited State 12:	Singlet-A	3.9786 eV	311.63 nm	$f=0.2803$	$\langle S^{*2} \rangle=0.000$
96 ->106	0.44692				
104 ->107	0.49200				
105 ->107	0.20010				
Excited State 15:	Singlet-A	4.3505 eV	284.99 nm	$f=0.0579$	$\langle S^{*2} \rangle=0.000$
94 ->106	-0.13756				
103 ->107	0.66263				
105 ->108	0.12371				
Excited State 17:	Singlet-A	4.4945 eV	275.86 nm	$f=0.2811$	$\langle S^{*2} \rangle=0.000$
94 ->106	0.59067				
101 ->107	0.12483				
103 ->107	0.15040				
105 ->108	-0.17464				
105 ->109	-0.19579				

Table S4: B3LYP TDDFT-predicted energies and expansion coefficients for compound **4** (only excited states with $f > 0.05$ and $\lambda > 270$ nm are listed).

Excited State 12:	2.785-A	2.3209 eV	534.20 nm	$f=0.0765$	$\langle S^{**2} \rangle = 1.688$
132A ->137A	0.26486				
133A ->137A	0.60604				
134A ->140A	-0.12426				
135A ->137A	0.26959				
136A ->137A	0.38617				
132B ->136B	0.34280				
133B ->136B	-0.13364				
134B ->136B	0.28425				
135B ->136B	-0.16384				
Excited State 13:	2.374-A	2.4084 eV	514.80 nm	$f=0.1838$	$\langle S^{**2} \rangle = 1.159$
132A ->137A	-0.32869				
133A ->137A	-0.18363				
135A ->137A	-0.29027				
136A ->137A	0.51979				
136A ->138A	-0.10332				
131B ->136B	0.22793				
132B ->136B	-0.22049				
133B ->136B	-0.36501				
134B ->136B	0.25270				
135B ->136B	-0.35812				
Excited State 21:	2.611-A	2.9470 eV	420.72 nm	$f=0.1167$	$\langle S^{**2} \rangle = 1.454$
131A ->137A	-0.13217				
132A ->137A	-0.47178				
133A ->137A	-0.11416				
136A ->138A	-0.11620				
129B ->136B	-0.10328				
130B ->136B	0.15923				
131B ->140B	0.21303				
132B ->136B	0.50229				
133B ->137B	0.11626				
134B ->137B	0.35201				
135B ->137B	-0.42651				
Excited State 22:	2.933-A	2.9792 eV	416.16 nm	$f=0.1352$	$\langle S^{**2} \rangle = 1.901$
129A ->137A	-0.15933				
131A ->137A	0.18525				
132A ->137A	-0.43366				
133A ->138A	0.15732				
135A ->137A	0.12112				
136A ->138A	0.36069				
128B ->136B	-0.11927				
129B ->136B	0.15826				
130B ->136B	-0.14897				

132B ->136B	0.40231				
133B ->137B	-0.11569				
135B ->137B	0.50777				
Excited State 27:	2.990-A	3.3015 eV	375.54 nm	f=0.0950	<S**2>=1.986
129A ->137A	-0.37287				
131A ->137A	0.26155				
132A ->137A	0.10719				
135A ->138A	-0.26136				
136A ->138A	0.28184				
127B ->136B	0.24347				
128B ->136B	-0.18783				
129B ->136B	0.16008				
132B ->136B	-0.12724				
133B ->137B	0.42969				
134B ->137B	0.25685				
135B ->137B	-0.32391				
Excited State 32:	2.978-A	3.4816 eV	356.12 nm	f=0.0946	<S**2>=1.968
125A ->137A	0.11821				
126A ->137A	0.19008				
128A ->137A	0.28974				
129A ->137A	-0.26413				
133A ->138A	-0.21570				
135A ->138A	0.45049				
136A ->138A	-0.31823				
126B ->136B	-0.28663				
127B ->136B	0.21566				
128B ->136B	-0.18491				
129B ->136B	0.22202				
130B ->136B	-0.11108				
133B ->137B	0.24949				
135B ->137B	0.14540				
Excited State 34:	2.331-A	3.5643 eV	347.85 nm	f=0.3552	<S**2>=1.109
126A ->137A	0.10762				
131A ->137A	-0.24184				
133A ->138A	0.15825				
134A ->138A	0.14319				
135A ->138A	0.36431				
136A ->138A	0.52475				
126B ->136B	-0.12094				
127B ->136B	0.11745				
130B ->136B	-0.12333				
132B ->136B	-0.13071				
132B ->137B	-0.12723				
133B ->137B	-0.33816				
134B ->137B	0.41460				
135B ->137B	-0.11129				

135B ->138B	-0.11156				
Excited State 39:	2.138-A	3.7010 eV	335.00 nm	f=0.2791	<S**2>=0.893
125A ->137A	0.14247				
128A ->137A	0.40104				
129A ->137A	-0.45890				
127B ->136B	-0.49361				
128B ->136B	0.51759				
Excited State 40:	3.153-A	3.7163 eV	333.62 nm	f=0.0729	<S**2>=2.235
125A ->137A	0.13577				
126A ->137A	-0.15285				
128A ->137A	0.10627				
128A ->138A	-0.10190				
129A ->137A	0.31526				
132A ->138A	-0.18054				
133A ->138A	0.31989				
135A ->138A	-0.11143				
135A ->139A	0.11924				
136A ->139A	-0.22569				
136A ->140A	0.14853				
136A ->141A	0.21535				
124B ->136B	-0.18240				
126B ->136B	-0.12674				
127B ->139B	0.11218				
129B ->136B	-0.11938				
133B ->137B	0.30546				
133B ->138B	-0.17212				
133B ->139B	0.17244				
135B ->138B	-0.20176				
135B ->139B	0.20156				

Table S5: B3LYP TDDFT-predicted energies and expansion coefficients for compound **3** (only excited states with $f > 0.05$ and $\lambda > 270$ nm are listed).

Excited State 5:	2.004-A	2.3456 eV	528.59 nm	$f=0.3010$	$\langle S^2 \rangle=0.754$
119A ->120A	0.69956				
118B ->119B	0.70259				
Excited State 12:	2.067-A	2.8461 eV	435.63 nm	$f=0.3752$	$\langle S^2 \rangle=0.818$
116A ->120A	0.18388				
118A ->120A	0.68381				
119A ->121A	0.13893				
117B ->119B	0.65881				
Excited State 26:	2.143-A	3.5332 eV	350.91 nm	$f=0.3358$	$\langle S^2 \rangle=0.898$
113A ->120A	0.30938				
119A ->121A	0.52709				
109B ->119B	0.17923				
112B ->119B	0.37356				
113B ->120B	0.23212				
117B ->119B	-0.12884				
117B ->121B	-0.16996				
118B ->121B	0.55269				
Excited State 29:	2.011-A	3.5752 eV	346.79 nm	$f=0.5110$	$\langle S^2 \rangle=0.761$
113A ->120A	0.57761				
119A ->121A	-0.33367				
112B ->119B	0.61157				
113B ->120B	-0.16013				
118B ->121B	-0.32950				
Excited State 31:	2.057-A	3.7582 eV	329.90 nm	$f=0.0810$	$\langle S^2 \rangle=0.808$
111A ->120A	-0.34604				
118A ->121A	0.10345				
119A ->121A	-0.14095				
97B ->120B	-0.12607				
109B ->119B	-0.11586				
110B ->120B	0.16399				
111B ->119B	-0.33941				
113B ->120B	0.75648				
117B ->121B	0.11008				
118B ->121B	-0.17835				
Excited State 32:	2.016-A	3.7908 eV	327.06 nm	$f=0.0623$	$\langle S^2 \rangle=0.766$
109A ->120A	-0.20685				
111A ->120A	0.61494				
119A ->121A	-0.10229				
109B ->119B	-0.10131				
110B ->120B	0.11666				
111B ->119B	0.56910				
113B ->120B	0.42505				

Excited State 36: 2.172-A 3.9645 eV 312.74 nm f=0.0823 <S**2>=0.929

109A ->120A	0.50418
111A ->120A	0.12638
118A ->121A	0.29162
108B ->119B	-0.16458
109B ->119B	0.57469
116B ->121B	0.11064
117B ->121B	0.42903

Excited State 40: 2.029-A 4.0378 eV 307.06 nm f=0.3370 <S**2>=0.779

108A ->120A	-0.13113
109A ->120A	-0.31193
118A ->121A	0.59298
119A ->121A	0.11805
109B ->119B	-0.32898
110B ->120B	0.10846
113B ->120B	-0.20414
117B ->121B	0.53710
118B ->121B	0.12619

Table S6: B3LYP TDDFT-predicted energies and expansion coefficients for compound **5** (only excited states with $f > 0.05$ and $\lambda > 270$ nm are listed).

Excited State 1:	Singlet-A	2.2998 eV	539.10 nm	$f=0.3175$	$\langle S^{*2} \rangle=0.000$
137 ->138	0.70435				
Excited State 2:	Singlet-A	2.8993 eV	427.63 nm	$f=0.3693$	$\langle S^{*2} \rangle=0.000$
136 ->138	0.67795				
137 ->139	0.15393				
Excited State 8:	Singlet-A	3.5090 eV	353.33 nm	$f=0.4289$	$\langle S^{*2} \rangle=0.000$
128 ->138	-0.43740				
136 ->138	-0.11440				
137 ->139	0.51376				
Excited State 9:	Singlet-A	3.5213 eV	352.10 nm	$f=0.3174$	$\langle S^{*2} \rangle=0.000$
128 ->138	0.52839				
136 ->138	-0.10473				
137 ->139	0.41969				
Excited State 10:	Singlet-A	3.6391 eV	340.70 nm	$f=0.3738$	$\langle S^{*2} \rangle=0.000$
130 ->138	0.68749				
Excited State 12:	Singlet-A	4.0062 eV	309.48 nm	$f=0.0669$	$\langle S^{*2} \rangle=0.000$
127 ->138	0.63824				
136 ->139	0.23401				
Excited State 13:	Singlet-A	4.0562 eV	305.67 nm	$f=0.2337$	$\langle S^{*2} \rangle=0.000$
127 ->138	-0.23395				
136 ->139	0.64242				
Excited State 15:	Singlet-A	4.2103 eV	294.47 nm	$f=0.0684$	$\langle S^{*2} \rangle=0.000$
137 ->140	0.62622				
137 ->141	-0.28431				
135 ->139	-0.16253				
Excited State 21:	Singlet-A	4.4883 eV	276.24 nm	$f=0.0888$	$\langle S^{*2} \rangle=0.000$
124 ->138	-0.14312				
125 ->138	0.48380				
133 ->139	0.42682				
Excited State 23:	Singlet-A	4.5644 eV	271.63 nm	$f=0.1585$	$\langle S^{*2} \rangle=0.000$
123 ->138	0.13534				
124 ->138	0.13912				
125 ->138	-0.38292				
133 ->139	0.50938				
137 ->141	0.10430				

Table S7: B3LYP DFT optimized geometry of compound **2**.

Center Number	Atomic Number	Atomic Type	Coordinates (Angstroms)		
			X	Y	Z
1	6	0	2.782980	4.459405	-0.000074
2	1	0	2.925576	5.530171	-0.000240
3	6	0	3.737891	3.439037	-0.000402
4	1	0	4.813435	3.519249	-0.000885
5	6	0	3.003344	2.246232	0.000021
6	6	0	2.791933	-0.100460	-0.000039
7	6	0	3.417048	-1.436440	-0.000153
8	6	0	4.739860	-1.861764	-0.000125
9	1	0	5.558811	-1.150650	-0.000160
10	6	0	4.974011	-3.241619	-0.000042
11	1	0	5.994504	-3.611123	-0.000018
12	6	0	3.913438	-4.158666	0.000026
13	1	0	4.130419	-5.221975	0.000113
14	6	0	2.584134	-3.723214	0.000002
15	1	0	1.758772	-4.426597	0.000056
16	6	0	2.361111	-2.350445	-0.000101
17	6	0	1.131977	-1.537903	0.000008
18	6	0	-1.213996	-1.535576	0.000004
19	6	0	-2.513076	-2.213207	0.000034
20	6	0	-2.828548	-3.569211	0.000144
21	1	0	-2.048523	-4.321942	0.000247
22	6	0	-4.179946	-3.917321	0.000135
23	1	0	-4.464469	-4.964133	0.000216
24	6	0	-5.180124	-2.932699	0.000027
25	1	0	-6.221992	-3.235456	0.000017
26	6	0	-4.859513	-1.573320	-0.000076
27	1	0	-5.629863	-0.810544	-0.000137
28	6	0	-3.511884	-1.229072	-0.000079
29	6	0	-2.852141	0.081043	-0.000150
30	6	0	-2.800435	2.427653	-0.000117
31	6	0	-3.459386	3.682185	-0.000323
32	1	0	-4.523839	3.854657	-0.000612
33	6	0	-2.442373	4.613336	-0.000087
34	1	0	-2.448715	5.692142	-0.000088
35	7	0	1.536815	3.962112	0.000495
36	7	0	1.690270	2.626229	0.000522
37	1	0	0.881184	2.016625	0.000872
38	7	0	3.510769	0.978653	-0.000064
39	7	0	1.391214	-0.226251	0.000087
40	7	0	-0.067867	-2.168297	0.000091
41	7	0	-1.473821	-0.191790	-0.000130
42	1	0	-0.754961	0.523785	-0.000199
43	7	0	-3.457806	1.214767	-0.000180
44	7	0	-1.457363	2.590151	0.000187
45	7	0	-1.278166	3.919615	0.000235
46	1	0	-0.306488	4.261623	0.000333

$E_h = -1340.432492$ Hartree

Table S8: B3LYP DFT optimized geometry of compound **4**.

Center Number	Atomic Number	Atomic Type	Coordinates (Angstroms)		
			X	Y	Z
1	6	0	-2.346697	-4.215028	0.269936
2	1	0	-2.361510	-5.292449	0.360639
3	6	0	-3.388028	-3.309595	0.176410
4	1	0	-4.453486	-3.481584	0.178723
5	6	0	-2.748848	-2.058851	0.081843
6	6	0	-2.786352	0.258199	-0.016240
7	6	0	-3.489566	1.540966	-0.068160
8	6	0	-4.841328	1.867341	-0.138580
9	1	0	-5.602461	1.095596	-0.177164
10	6	0	-5.176956	3.222868	-0.159579
11	1	0	-6.220723	3.515393	-0.215894
12	6	0	-4.187303	4.218716	-0.109202
13	1	0	-4.483484	5.262731	-0.126615
14	6	0	-2.833590	3.885359	-0.037887
15	1	0	-2.063582	4.647954	0.001322
16	6	0	-2.506285	2.531117	-0.018218
17	6	0	-1.221247	1.834369	0.045210
18	6	0	1.087125	1.905251	0.044322
19	6	0	2.335264	2.673239	0.062699
20	6	0	2.589186	4.039940	0.141982
21	1	0	1.779041	4.757229	0.213417
22	6	0	3.925494	4.446896	0.128632
23	1	0	4.165297	5.503562	0.190746
24	6	0	4.967784	3.510862	0.036386
25	1	0	5.995316	3.860263	0.028503
26	6	0	4.703987	2.140884	-0.044206
27	1	0	5.505148	1.413244	-0.114747
28	6	0	3.370848	1.743447	-0.029175
29	6	0	2.736143	0.422223	-0.088695
30	6	0	2.836911	-1.889110	-0.172779
31	6	0	3.539199	-3.111841	-0.269120
32	1	0	4.606655	-3.225930	-0.368359
33	6	0	2.569110	-4.088299	-0.197947
34	1	0	2.626177	-5.165525	-0.222646
35	6	0	0.437209	-1.872383	3.111066
36	1	0	-0.178529	-2.750452	2.898316
37	1	0	0.386490	-1.626338	4.175164
38	1	0	1.469969	-2.079344	2.838635
39	6	0	0.001975	-2.013752	-3.060863
40	1	0	1.008624	-2.441731	-3.042460
41	1	0	-0.293604	-1.803988	-4.092581

42	1	0	-0.699098	-2.717823	-2.618436
43	27	0	0.007137	-0.852720	0.022118
44	7	0	-1.163608	-3.566586	0.232306
45	7	0	-1.389195	-2.237822	0.114636
46	7	0	-3.410466	-0.872508	-0.007272
47	7	0	-1.398950	0.489406	0.051256
48	7	0	-0.082379	2.522028	0.079195
49	7	0	1.342547	0.569428	-0.043308
50	7	0	3.433868	-0.664445	-0.168386
51	7	0	1.500779	-2.127888	-0.052952
52	7	0	1.377917	-3.469856	-0.071929
53	1	0	0.382337	-3.821702	0.055815
54	8	0	0.029925	-0.747022	2.316336
55	8	0	-0.075113	-0.821809	-2.264741
56	1	0	0.546853	-0.170320	-2.613333
57	1	0	-0.864434	-0.493907	2.579161

$E_h = -2953.612817$ Hartree

Table S9: B3LYP DFT optimized geometry of compound **3**

Center Number	Atomic Number	Atomic Type	Coordinates (Angstroms)		
			X	Y	Z
1	6	0	-2.558415	4.350422	0.001502
2	1	0	-2.611733	5.427912	0.002072
3	6	0	-3.540974	3.379134	0.000905
4	1	0	-4.611388	3.506584	0.000860
5	6	0	-2.845944	2.151299	0.000390
6	6	0	-2.772017	-0.174885	-0.000135
7	6	0	-3.420713	-1.493477	-0.000541
8	6	0	-4.757796	-1.874524	-0.001094
9	1	0	-5.551815	-1.136088	-0.001378
10	6	0	-5.035378	-3.244628	-0.001267
11	1	0	-6.066954	-3.581432	-0.001694
12	6	0	-4.003972	-4.196181	-0.000893
13	1	0	-4.255550	-5.251665	-0.001035
14	6	0	-2.662621	-3.805492	-0.000342
15	1	0	-1.859486	-4.533791	-0.000059
16	6	0	-2.395437	-2.439748	-0.000168
17	6	0	-1.134708	-1.688046	0.000354
18	6	0	1.185265	-1.658799	0.000565
19	6	0	2.459058	-2.380935	0.000676
20	6	0	2.756119	-3.741974	0.001010
21	1	0	1.968227	-4.486828	0.001410
22	6	0	4.103937	-4.104443	0.000836
23	1	0	4.378333	-5.154262	0.001114
24	6	0	5.115294	-3.129729	0.000291
25	1	0	6.153817	-3.444872	0.000136
26	6	0	4.810129	-1.766693	-0.000081
27	1	0	5.589611	-1.012852	-0.000506
28	6	0	3.464756	-1.410299	0.000119
29	6	0	2.788768	-0.110018	-0.000242
30	6	0	2.792131	2.222563	-0.001044
31	6	0	3.455596	3.461945	-0.001732
32	1	0	4.523983	3.614141	-0.002403
33	6	0	2.431844	4.397596	-0.001396
34	1	0	2.475015	5.477843	-0.001658
35	29	0	0.003042	1.074077	0.000194
36	7	0	-1.367778	3.723382	0.001428
37	1	0	-0.365273	4.064840	0.000861
38	7	0	-1.506492	2.384603	0.000674
39	7	0	-3.450908	0.924295	-0.000180
40	7	0	-1.379663	-0.349477	0.000392
41	7	0	0.027582	-2.321771	0.000722
42	7	0	1.396630	-0.323140	0.000112
43	7	0	3.425288	1.012768	-0.000850
44	7	0	1.439187	2.443266	-0.000298
45	7	0	1.235509	3.778035	-0.000513

 $E_h = -2979.786503$ Hartree

Table S10: B3LYP DFT optimized geometry of compound **5**.

Center Number	Atomic Number	Atomic Type	Coordinates (Angstroms)		
			X	Y	Z
1	6	0	2.818163	-4.071130	0.029343
2	1	0	2.944761	-5.142343	0.048662
3	6	0	3.733809	-3.036943	-0.031094
4	1	0	4.809294	-3.105112	-0.070387
5	6	0	2.960299	-1.849502	-0.027661
6	6	0	2.750884	0.501655	-0.071081
7	6	0	3.339774	1.854782	-0.095886
8	6	0	4.656114	2.300654	-0.128022
9	1	0	5.483436	1.599427	-0.142668
10	6	0	4.872466	3.682392	-0.140876
11	1	0	5.887625	4.065567	-0.165993
12	6	0	3.798961	4.584557	-0.121326
13	1	0	4.000520	5.650905	-0.131313
14	6	0	2.477125	4.130433	-0.088839
15	1	0	1.641782	4.821858	-0.073047
16	6	0	2.268972	2.755062	-0.076358
17	6	0	1.037927	1.943164	-0.046075
18	6	0	-1.311598	1.823970	-0.010026
19	6	0	-2.615749	2.504878	-0.008535
20	6	0	-2.967225	3.851879	-0.019412
21	1	0	-2.208299	4.626702	-0.029171
22	6	0	-4.328336	4.166691	-0.016297
23	1	0	-4.640327	5.206195	-0.023889
24	6	0	-5.302235	3.156434	-0.003103
25	1	0	-6.352199	3.431962	-0.001241
26	6	0	-4.944434	1.805235	0.007697
27	1	0	-5.696557	1.023645	0.017978
28	6	0	-3.588327	1.494166	0.004520
29	6	0	-2.860042	0.214830	0.015970
30	6	0	-2.795233	-2.154653	0.059825
31	6	0	-3.441167	-3.407466	0.059214
32	1	0	-4.506375	-3.582956	0.036807
33	6	0	-2.402438	-4.330322	0.093783
34	1	0	-2.440854	-5.411568	0.105099
35	6	0	0.019924	-2.117926	-3.085223
36	1	0	1.034058	-2.500687	-3.232398
37	1	0	-0.433493	-1.884236	-4.052206
38	1	0	-0.580197	-2.866027	-2.572124
39	6	0	0.995342	-0.907037	3.244700
40	1	0	1.626665	-1.800324	3.249910
41	1	0	0.591669	-0.730996	4.245293

42	1	0	1.588535	-0.047147	2.940290
43	1	0	-0.635216	-1.767488	2.520169
44	1	0	0.571544	-0.271436	-2.627618
45	7	0	1.586863	-3.514022	0.067221
46	1	0	0.628311	-3.919297	0.105212
47	7	0	1.648759	-2.173037	0.032621
48	7	0	3.478977	-0.573382	-0.068954
49	7	0	1.359891	0.622505	-0.045947
50	7	0	-0.159521	2.518503	-0.030263
51	7	0	-1.487085	0.494209	0.004886
52	7	0	-3.444277	-0.942220	0.035714
53	7	0	-1.443232	-2.366610	0.096903
54	7	0	-1.206024	-3.698992	0.117294
55	8	0	0.019363	-0.959866	-2.236551
56	8	0	-0.066701	-1.022053	2.287481
57	30	0	-0.010477	-0.916159	0.023581

$E_h = -3350.167009$ Hartree

References

- 1 I.-S. Tamgho, J. T. Engle and C. J. Ziegler, *Tetrahedron Lett.*, 2013, **54**, 6114–6117.
- 2 G. M. Sheldrick, *Acta Crystallogr. Sect. A Found. Crystallogr.*, 2008, **64**, 112–122.
- 3 P. J. Stephens, F. J. Devlin, C. F. Chabalowski and M. J. Frisch, *J. Phys. Chem.*, 1994, **98**, 11623–11627.
- 4 J. Tomasi, B. Mennucci and R. Cammi, *Chem. Rev.*, 2005, **105**, 2999–3093.
- 5 A. D. McLean and G. S. Chandler, *J. Chem. Phys.*, 1980, **72**, 5639–5648.
- 6 M. J. Frisch, G. W. Trucks, H. B. Schlegel, G. E. Scuseria, Ma. Robb, J. R. Cheeseman, G. Scalmani, V. Barone, B. Mennucci and G. A. Petersson, *Inc. Wallingford, CT*.
- 7 Tenderholt, Adam L. *QMForge*, Version 2.4, <https://qmforge.net>